ISSN 0031-918X, The Physics of Metals and Metallography, 2013, Vol. 114, No. 3, pp. 266–271. © Pleiades Publishing, Ltd., 2013.
Original Russian Text © M.P. Kashchenko, V.G. Chashchina, 2013, published in Fizika Metallov i Metallovedenie, 2013, Vol. 114, No. 3, pp. 290–296.

STRENGTH AND PLASTICITY

Estimation of the Effective Growth Rate of a Plate of Bainitic Ferrite in Dynamic Theory

M. P. Kashchenko[a, b] **and V. G. Chashchina**[b]
[a] *Ural State Institute of Forestry Engineering, Sibirskii tract 37, Ekaterinburg, 620100 Russia*
[b] *Yeltsin Ural Federal University, ul. Mira 19, Ekaterinburg, 620002 Russia*
e-mail: mpk46@mail.ru

Received July 6, 2012

Abstract—The growth of a bainite plate is considered to be a relay-type process, in which fast (with $\tau_g \sim 10^{-10}$ s) acts of the formation of sublaths (with a width $3d \sim 1$ μm, where d is the thickness of the sublath) occur in an ultrasonic regime and the successive acts are separated by pauses of length $\tau_p \sim 10^{-2}$ s. The value τ_p corresponds to the time of diffusion on a scale d with allowance for the pipe diffusion. The effective growth rate of the plate of bainite ferrite v_{eff} is estimated by the relationship $3d/\tau_p$.

Keywords: bainitic transformation, dynamic theory, carbon diffusion, incubation periods, bainite growth rate
DOI: 10.1134/S0031918X13030101

1. INTRODUCTION

In steels, bainite is the product of the transformation of overcooled austenite at temperatures at which the self-diffusion in iron is almost completely suppressed, but carbon diffusion is still quite significant. Bainite arises in the form of clusters of ferrite crystals of platelet or lath shape with interlayers of cementite and retained austenite. In turn, the crystals of bainitic ferrite can consist of finer subcrystals. Below, we mainly consider steels with relatively low concentrations of carbon (to 0.6 wt %), in which the bainitic transformation results in the formation of a mixture of relatively fine laths that include fine carbide particles (lower, or low-temperature, bainite). For the sake of comparison, one should mind that upper, or high-temperature, bainite consists of relatively coarse ferrite laths that alternate with interlayers of iron carbide. The lath component of the lower bainite resembles the laths of packet martensite formed upon quenching austenite to lower temperatures, at which the carbon diffusion also is nearly suppressed (in more detail, the problem of bainitic and martensitic transformations is described, e.g., in [1–4]).

From the viewpoint of the theory of solid solutions, martensite is ferrite supersaturated with carbon with the same concentration of carbon as in the case of austenite and with a degree of supersaturation that exceeds its concentration in the bainitic ferrite (in ferrite, significant supersaturation may not exist). When speaking of the morphological signs of the lath components of bainite and martensite, it should be noted that, in both cases, except for the similarity of crystal shapes (and habits close to $\{hh\ell\}_\gamma$ type), similarity is also observed in the appearance of a surface relief, which indicates the formation of a macroshift in the region of the lath crystal, as well as in the interphase orientation relationships (ORs). The presence of these closely related morphological signs is typical of the cooperative variant of transformation according to the martensitic mechanism [2]; therefore, there are grounds for considering the lath components of bainite to be crystals that are formed (at least at the first stage) according to a mechanism analogous to the case of laths of packet martensite.

The succession of the manifestation of the carbon mobility in the course of a bainitic transformation is described in the literature by at least two extreme variants.

(1) The lath components of bainite are formed in the austenite regions preliminarily depleted of carbon (see, e.g., [1–3]). Then, the chemical composition of the steel in these regions corresponds to a higher temperature of the onset of the martensitic transformation $M_s(c_b)$ as compared to the temperature $M_s(c_a)$ of the initial austenite with a uniform distribution of carbon over the volume of the sample as follows: $c_b < c_m = c_a$, where c_b, c_m, and c_a are the carbon concentrations in the laths of bainite and martensite and in the initial austenite, respectively.

(2) The plates of bainitic ferrite are formed according to a diffusionless mechanism in the initial austenite; after this, carbon diffuses from the carbon-supersaturated ferrite into the retained austenite, forming carbide interlayers, which is typical of upper bainite. In the lower bainite, fine fractions of carbides are formed inside ferrite plates, along with carbide interlayers [4].

It is noted in [1–3] and [4] that, regardless of the sequence in which the redistribution of carbon occurs, a substantial decrease takes place in the rate of growth of bainitic ferrite as compared to the growth rate of martensite. Two variants for the explanation of the decrease in the growth rate of bainitic ferrite appear to be possible. The first is based on the continuous character of growth synchronized with the diffusion process. This scenario can be implemented if the bainite growth is interpreted based on the motion of transformation dislocations (the various cases of this motion are discussed qualitatively in [5]). The second variant is based on a discrete character of growth, although it visually is taken as a relatively slow, continuous process. In reality, this type of growth can represent a sequence of fast (supersonic) but short jumpwise acts of growth of a ferrite crystal. Carbides are formed during the long (as compared to the jump time) stopping intervals (pauses between growth acts). This approach is close to that considered in [6].

The aim of this work is to show the similarity of the mechanisms of the formation of lath crystals of bainite and of packet martensite in terms of the dynamic theory of the formation of martensite crystals [7–9] based on experimental information concerning the morphological signs of bainitic ferrite, as well as to give an adequate interpretation of the effective rate of growth of a bainitic-ferrite plate.

2. BASIC CONCEPTS OF THE DYNAMIC APPROACH TO THE FORMATION OF MARTENSITE CRYSTALS IN STEELS

One should note that a specific feature of the γ–α martensitic transformation (MT) in steels is an extremely high (supersonic) rate of crystal growth, which is adequately described [7–9] in terms of the concept of the control wave process (CWP). The wave mechanism of controlling growth is associated with the specific process of heterogeneous nucleation of crystals, which is related to the appearance of an initial excited (oscillatory) state (in the form of an elongated rectangular parallelepiped) in the elastic field of a defect (as a rule, of an individual dislocation). Pairs of wave beams that propagate from the region of the excited state initiate the tension–compression-type threshold deformation in orthogonal directions $\mathbf{n}_{1,2}$, which are specified by the eigenvectors $\xi_{1,2}$ of the deformation tensor of the elastic field of the defect in the region of the appearance of the initial excited state (IES).

It can easily be shown [7, 9] that the normal $\mathbf{N}_w$ to the habit plane, which is related to the propagation of the CWP, is specified by the relationship

$$\mathbf{N}_w \parallel \mathbf{n}_2 \pm \mathbf{n}_1\kappa, \quad \kappa = v_2/v_1, \quad \mathbf{n}_1 \perp \mathbf{n}_2, \quad |\mathbf{n}_i| = 1, \qquad (1)$$

where v_1 and v_2 are the absolute values of the velocities of the wave propagation in the directions $\mathbf{n}_1$ and $\mathbf{n}_2$.

It is also important that, in the case of single crystals and coarse grains, the magnitude d of the transverse dimension of the IES is on the order of one hundredth of the dimension L, which specifies the dimensions of the defect-free (mainly, dislocation-free) zone. The requirement

$$d \approx 10^{-2}L \qquad (2)$$

reflects (in accordance with Fig. 1) two conditions: first, the distance from the dislocation-related nucleation center to the site of the localization of the excited (oscillatory) state is $r \approx 10^{-1}L$, which guarantees the domination of the elastic field of an individual dislocation, and, second, d is $\sim 10^{-1}r$, which guarantees the validity of the continuum calculation (performed for the angle θ_0) in the range of the angular localization $\Delta\theta$ for the region of the excited state.

As was shown in [10], at the initial stage of the formation of crystals of packet martensite, segments of dislocation loops oriented along the most closely packed directions $\langle 110\rangle_\gamma$ play the main role; furthermore, directions $\xi_{1,2}$ are chosen, which are close to the orthogonal fourfold and twofold axes that correspond to the region with the extremal values of deformations, where the thresholds for fluctuations that lead to the appearance of a CWP are reduced to the greatest extent. As was shown by careful measurements [11], ORs for the lath martensite are close to Nishiyama's values, which can naturally be explained in terms of the dynamic approach [12]. The habit planes of the laths are close to $\{\tilde{5}57\}_\gamma$, where the tilde sign marks the index that, of the two close Miller indices, is arbitrary greater. The exact coincidence of the pair of Miller indices in the case of the wave description of the habit plane is achieved for the edge orientation of the Burgers vector with respect to the dislocation line $\langle 110\rangle_\gamma$. However, in the case of a mixed orientation (60° dislocation), different, though close, values of this pair of indices of habit planes are naturally obtained. As it is shown in [10], this leads to an increase in the degeneracy of the orientations, which corresponds to the most typical pattern [13], where to each packet there corresponds up to six orientations of the morphological signs (in particular, a concrete triangle in the stereographic projection corresponds to each orientation of the normal to the habit plane).

In the case of a lath shape of a martensite crystal, the stage of fast growth specifies the width of the crystal, whose thickness is less (although is of the same order) than the half-length of the waves in the CWP that are responsible for describing the habit planes. The laths of packet martensite are formed in a relatively high-temperature range (as compared to the conditions of the formation of plate-type martensite). Therefore, because of the strong phonon attenuation, the fulfillment of the regime of the generation of control waves by nonequilibrium electrons (in the interphase region at the growth stage) is not achieved.

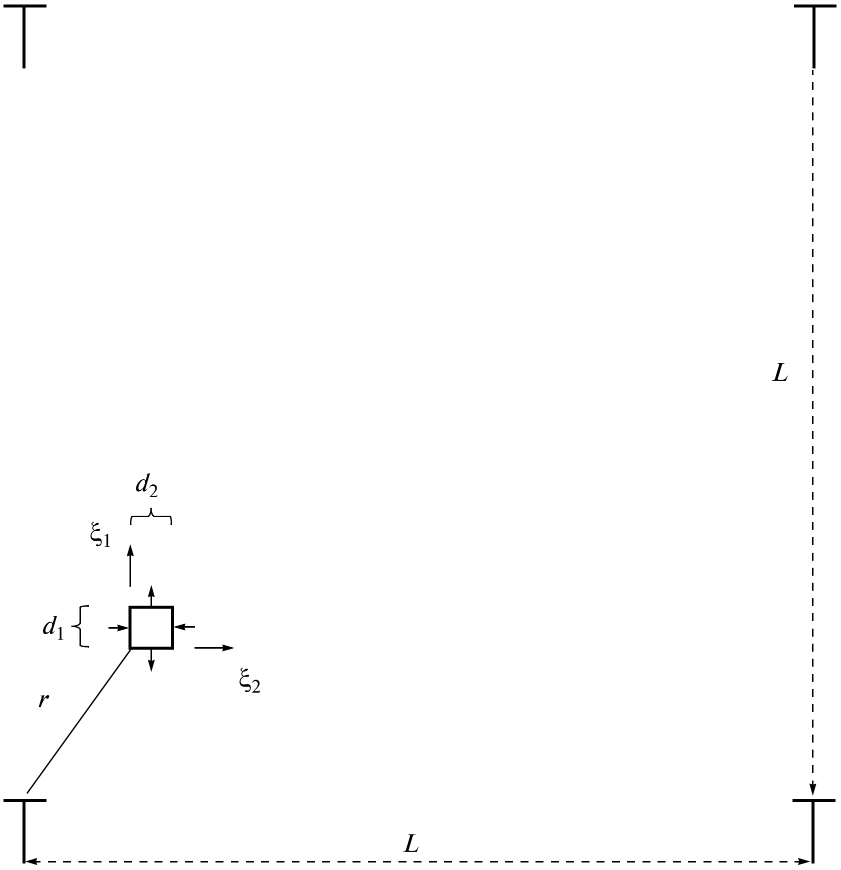

Fig. 1. Relationship of spatial scales upon appearance of initial excited state (IES) in the elastic field of a dislocation (schematic).

As a result, in the case of lath crystals, the overthreshold regime of growth is realized at the expense of the initial amplitudes of oscillations and breaks off, as soon as the wave amplitudes decrease to below the threshold values. Therefore, it is not a mere chance that the width of the lath often only moderately exceeds its thickness.

3. SPECIFIC FEATURES OF MORPHOLOGY OF BAINITIC LATH FERRITE

At first sight (upon a rough description based on the data of optical microscopy), as was already noted, the observed morphology of upper bainite that contains more coarse (than in the case of lower bainite and martensite) laths does not correspond to the mechanism of the wave growth of martensite laths. Indeed, at higher temperatures, the phonon attenuation becomes still more pronounced and the lath widths should decrease, rather than increase. Naturally, this only refers to a comparison of the attenuation of phonons with equal wavelengths λ. However, when comparing the attenuation of waves with different λ, long-wavelength shifts should exhibit smaller attenuations. Therefore, the coarsening of laths of upper bainite could be interpreted as a consequence of the participation of waves with longer λ in the control of crystal growth. However, this simple scaling is still insufficient to reflect the entire range of existing features of morphology upon passing from a general to more detailed description (based on the data of transmission electron microscopy). According to [4], in addition to laths that have no fine structure, there are also relatively coarse laths, which are formed as a result of the merging of sublaths of about 0.1 μm thick with interlayers of retained austenite in between them.

The data on the habits of bainitic laths available in the literature differ substantially, remaining close to the $\{hh\ell\}_\gamma$ type. Thus, Bhadeshia [4] mentions $\{558\}_\gamma$ habits; the habits measured in [14] for lower bainite are close to $\{335\}_\gamma$, while those measured in [15] for upper bainite are close to $\{223\}_\gamma$.

A common feature of the above results is that the ratio of the indices l to h exceeds the value 7/5 (~1.4) typical of the habit of packet martensite. This is related, first, to the difference in the alloy composition, which leads to a difference in the elasticity moduli and in the ratios κ of the velocities of control waves in (1); and, second, to the change in the orientations of vectors $\boldsymbol{\xi}_{1,\,2}$ (and, consequently, $\mathbf{n}_{1,\,2}$ in (1)) in the region of the localization of IESs. The latter circumstance can be caused by the redistribution of carbon atoms in the elastic fields of defects, which can lead to the modification of the elastic field of the dislocation-related nucleation center (DNC) and, correspondingly, to displacements of the region of the spatial localization of the IES.

Another important feature, which was emphasized in [4] and is based on the data of [16], is related to the bimodal character of the habit of sublaths that enter into the composition of macroplates of bainitic ferrite. Along with the sublaths that exhibit $\{hh\ell\}_\gamma$ habits with $h < \ell$, habits are also observed with $h > \ell$, namely, $\{0.373\ 0.663\ 0.649\}_\gamma$ with ORs close to the Nishiyama OR. In the approximation of small integer indices, these habits occupy a position that is intermediate between $\{477\}_\gamma$ and $\{599\}_\gamma$. Sandvik [16] also noted the presence of numerous austenite twins that accompany the appearance of bainite. This gives us grounds to interpret the $\{477\}_\gamma$ habit as $\{855\}_\gamma$ analogs, but in the crystallographic basis of twinned austenite. Another interpretation of $\{477\}_\gamma$ habits is related to the modification of the elastic field of a DNC due to the compressive elastic field produced in austenite by sublaths with $\{855\}_\gamma$ habits. A further concretization of the above possibilities is insignificant for the aims of this work. One should note that the leading role in the bimodal composition of the plate of bainitic ferrite belongs to laths with $\{hh\ell\}_\gamma$ habits with $h < \ell$. As is shown in Fig. 2 (corresponding to a fragment of Fig. 2.3 in [4]), the formation of a plate of bainitic ferrite starts from a thin sublath and the orientation of one of the plate boundaries is determined by the orientation of analogous sublaths. It is important that the observed morphology of the plate suggests the relay mechanism of its formation from sublaths.

4. ESTIMATION OF CHARACTERISTIC TIMES AND EFFECTIVE GROWTH RATE OF A PLATE OF BAINITIC FERRITE

For bainitic ferrite, the presence of morphological signs uniquely related between themselves is typical of the cooperative variant of the transformation according to a martensitic mechanism. Therefore, it is assumed that the second scenario mentioned at the end of the introduction is the one that occurs in reality; i.e., individual laths and sublaths of bainitic ferrite are formed according to the diffusionless mechanism and their fast growth is adequately described in terms of the control wave process (CWP). The formation of a composite plate of bainitic ferrite has a relay character and the incubation time τ_p (pause) between successive starts of sublath growth in the general case does not coincide with the time τ_i of the initiation of the bainite reaction after quenching to temperatures $B_s = M_s(c_b) > M_s(c_a)$. During the incubation period τ_i, the first stage of the redistribution of carbon occurs. As a result, as was noted above, the formation of lath components of bainite occurs in the austenite regions that were preliminarily depleted of carbon. The subsequent stages of carbon redistribution are related to both the creation of additional carbon-depleted austenite regions and to the diffusion of carbon from the supersaturated ferrite into the retained austenite with the formation of carbide precipitates.

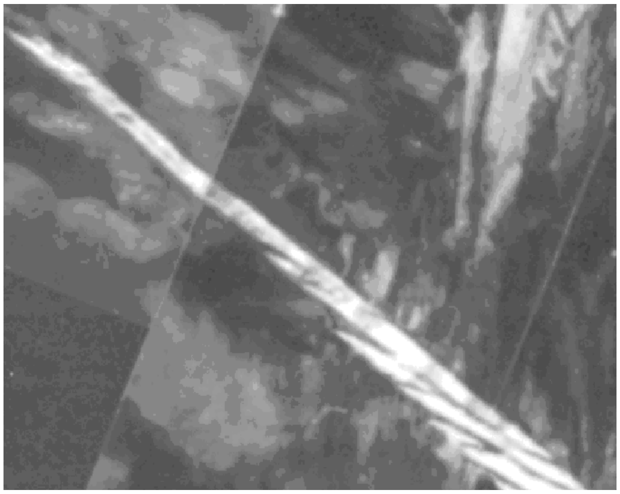

Fig. 2. Portion of a bainitic-ferrite plate with a bimodal composition of sublaths (given by white) [4, fragment of Fig. 2.3].

If, in the course of successive short-time acts of growth (with a supersonic velocity for some time τ_g), isolated laths separated by relatively long pauses τ_p are united into platelike regions, the growth of these regions visually appears to be a relatively slow and continuous growth with some effective velocity v_{ef}. Velocity v_{ef} refers to the velocity of growth of the greatest dimension of the plate (the effective velocity of the thickening of bainitic ferrite is not considered here).

Let us show that the duration of the pause between two successive acts of lath formation is both much longer than the time of growth of an isolated lath and much shorter than the incubation period as follows:

$$\tau_g \ll \tau_p \ll \tau_i. \tag{3}$$

Let us estimate the characteristic times that enter into (3) in terms of the CWP concept.

(1) Let the dimensions of the lath be related to one another as 1 : 3 : 10, i.e., be similar to those for lath martensite [17], and take into account that the lath thickness is less than, but is close to half the wavelength λ_Δ of the longitudinal waves propagating along the fourfold symmetry axis. Then, $\tau_g \approx 3\lambda_\Delta/2v$, where $v \approx v_\Delta\sqrt{2}$, and v_Δ is the corresponding velocity of longitudinal waves. Consequently, $\tau_g \approx T_\Delta$, where T_Δ is the period of oscillations with a wavelength λ_Δ. At $\lambda_\Delta \approx 1$ μm and $v_\Delta \approx 5 \times 10^3$ m/s, we obtain $T_\Delta \approx 2 \times 10^{-10}$ s.

(2) The minimum necessary scale of time that specifies the incubation period τ_i is determined by the time of bulk diffusion (with a carbon diffusion coefficient $D(B_s)$) at the temperature $B_s = M_s(c_b)$ of the beginning of growth of bainitic ferrite, which requires the carbon concentration to be decreased on the scale of the order of the transverse dimension d of the arising IES. Consequently,

$$\tau_i \sim d^2/4D(B_s) \approx (\lambda_\Delta/2)^2/4D(B_s). \qquad (4)$$

At the value of the specific energy of activation for carbon in steel $Q = 31.5$ kkal/mol $= 133.56$ kJ/mol, the preexponential factor $D_0 = 5 \times 10^{-6}$ m^2/s, and $B_s = 700$ K, we find from the formula

$$D(T) = D_0 \exp(Q/RT), \qquad (5)$$

where $R = 8.31$ J/mol, and $D(B_s) \approx 5 \times 10^{-16}$ m^2/s. Then, Eq. (4) yields the following estimate: $\tau_i \sim 10^2$ s, i.e., a value on the order of a few minutes. Note that the decrease in B_s to 600 K (at the other parameters being unaltered) increases τ_i by a factor of 50.

(3) Since the temperature is relatively high, the act of jumpwise growth in the lath (and sublaths) should be accompanied by significant stresses and by their intense relaxation in the adjacent austenite due to the formation of dislocations (just as inside the lath). This freshly formed dislocation structure is capable of sharply increasing the diffusion coefficient of carbon, which leads to the decarburization of the near zone of the arising lath, which stimulates the formation of carbide in austenite. To initiate lath growth, it is sufficient (just as upon the completion of the incubation period) to have a zone with a transverse section $d \sim (\lambda_\Delta/2)$ that is free of carbon. Then, the time τ_p is estimated from a relationship analogous to (4) as follows:

$$\tau_p \sim d^2/4D_{ef}(B_s), \qquad (6)$$

where $D_{ef}(B_s)$ is the effective coefficient of carbon diffusion that takes into account also diffusion along dislocation cores. This treatment is supported by the sharp increase in the rate of bainitic reaction over the course of plastic deformation [3], when the freshly formed dislocations, which had no time to become saturated by carbon, play the role of pipes that exhibit enhanced diffusion coefficient. If, as is permitted in the estimates based on the literature data, we assume that the magnitude of $D_{ef}(B_s)$ is on the order of the coefficient of bulk diffusion at a temperature of 1000°C, we obtain $D_{ef}(B_s) \sim 10^{-11}$ m^2/s. With the formal use of Eq. (5), this means that the motion along dislocation cores is related to a decreased (by a factor of about two) activation energy; therefore, the twofold decrease in temperature does not affect the magnitude of D. Naturally, upon the diffusion of carbon along dislocation cores, the coefficient D_{ef} can depend on temperature more weakly than in traditional form (5). If $D_{ef}(B_s) \sim 10^{-11}$ m^2/s, we find from (6) that $\tau_p \sim 6 \times 10^{-3}$ s. Since $\tau_p \gg \tau_g$, the magnitude of the effective rate v_{ef} is estimated by the ratio of the lath width to τ_p ($v_{ef} \sim 3d/\tau_p$). At $d \approx 0.5$ μm, we have $v_{ef} \sim 4 \times 10^2$ μm/s.

5. DISCUSSION

(1) The above estimates appear to correctly reflect the orders of magnitudes. Thus, e.g., the value of the velocity of bainite growth given in [4] (≈78 μm/s) can easily be obtained by assuming the value $d_1 \approx 0.221$ μm (instead of the above-taken value $d \approx 0.5$ μm), which does not contradict the observed thicknesses of sublaths.

(2) We would like to draw attention of researchers to the performance of simple experiments in order to verify the suggested picture of the formation of a bainitic transformation and obtain additional information. Indeed, using filming with a frame rate of no less than 10^3 s^{-1}, one can measure the values of τ_p, after which, by measuring the lath thickness d (using optical metallography), we can easily find v_{ef}. The measurement of v_{ef} permits one to compare the experimental values with the calculated results. On the other hand, measurements of v_{ef}, d, and τ_p makes it possible to find the values of $D_{ef}(B_s)$ for any steel composition (at a concrete temperature B_s). Note that, in this case, the determination of the coefficient of pipe diffusion proves to be rather natural, since the freshly formed dislocations have cores that have not yet been saturated by carbon. Consequently, based on the phenomenon of a bainitic transformation, the independent method of measuring the coefficient of pipe diffusion can be suggested.

(3) Similarly, the data on the duration of τ_i can be used in the analysis of the values of the coefficient of bulk diffusion $D(B_s)$, which mainly depends on temperature and alloy composition (which affects the activation energy of diffusion). Naturally, for a more realistic description, the effect of elastic fields of defects should be taken into account.

(4) The fact that adequate agreement with the experiment can be obtained based on a single scale d indicates the directional character of diffusion in the field of a rectilinear segment of a dislocation line (or a line of intersection of dislocation loops that are gliding in intersecting slip planes). In the elastic field of these segments, an IES arises in the form of an elongated rectangular parallelepiped.

(5) It should be emphasized that the central role in the above consideration (as, in general, in the theory of reconstructive martensitic transformations) belongs to the concept of the initial excited state (IES) and the magnitude d of the transverse dimension of the IES, which specifies the characteristic spatial scale used to calculate the time of diffusion. Here, it is appropriate to note that the knowledge of d allowed us [18, 19] to perform estimates of critical rates of cooling for the first time that agree with experiment [5]. It is interest-

ing that, in [18, 19], the physical formulation of the problem was related to the suppression of diffusion on scale d, whereas in this work, we used the inverse requirement, i.e., the realization of diffusion on the scale d.

ACKNOWLEDGMENTS

We are grateful to the participants in the 20th St. Petersburg Readings on Strength Problems for a fruitful discussion of the results briefly presented in [20].

REFERENCES

1. M. E. Blanter, *Phase Transformations upon Heat Treatment of Steel* (Metallurgizdat, Moscow, 1962) [in Russian].
2. G. V. Kurdyumov, L. M. Utevskii, and R. I. Entin, *Transformations in Iron and Steel* (Nauka, Moscow, 1977) [in Russian].
3. M. L. Bernshtein, V. A. Zaimovskii, and L. M. Kaputkina, *Thermomechanical Treatment of Steel* (Metallurgiya, Moscow, 1983) [in Russian].
4. H. K. D. H. Bhadeshia, *Bainite in Steels: Transformation, Microstructure and Properties* 2nd Ed. (Institute of Materials, London, 2001).
5. D. A. Mirzaev, M. M. Shteinberg, T. N. Ponomareva, and V. M. Schastlivtsev, "Effect of the Cooling Rate on the Martensite-Point Position. II. Alloy Steels," Fiz. Met. Metalloved. **47**, 986–992 (1979).
6. J. M. Oblac and R. F. Hehemann, *Transformations and Hardenability in Steels* (Climax Moly, Ann Arbor, 1967).
7. M. P. Kashchenko and V. G. Chashchina, "Dynamic Model of Supersonic Martensitic Crystal Growth" Phys.-Usp. **54**, 331–349 (2011).
8. M. P. Kashchenko and V. G. Chashchina, "Formation of Martensite Crystals in the Limiting Case of the Supersonic Rate of Growth," Pis'ma Mater. **1**, 7–15 (2011).
9. M. P. Kashchenko and V. G. Chashchina, *Dynamical Model of the γ–α Transformation and a Solution to the Critical Grain Size Problem* (NITs Regul. i Khaotich. Dinamika, Izhevsk. Inst. Komp'yuternykh Issledovanii, Izhevsk, 2010) [in Russian].
10. M. P. Kashchenko, *Wave Model of Martensite Growth upon the γ–α Transformation in Iron-Based Alloys*, 2nd Ed. (NITs Regul. i Khaotich. Dinamika, Izhevsk. Inst. Komp'yuternykh Issledovanii, Izhevsk, 2010) [in Russian].
11. B. P. J. Sandvik and C. M. Wayman, "Electron Microscopy Studies of Lath Martensite," J. Phys. (France) **43**, 557–562 (1982).
12. V. G. Chashchina, "A γ–α Martensite Transformation during the Fastest Rearrangement of the $\{110\}_\gamma$ Planes," Russ. Phys. J. **52**, 766–768 (2009).
13. V. M. Schastlivtsev and D. A. Rodionov, *Steel Single Crystals* (UrO RAN, Ekaterinburg, 1996) [in Russian].
14. C. P. Luo and J. Liu, "Crystallography of Lath Martensite and Lower Bainite in Alloy Steels," Mater. Sci. Eng., A **438–440**, 149–152 (2006).
15. A. T. Davenport, "The Crystallography of Upper Bainite," Republic Steel Res.. Rep. on Project 12051, pp. 1–35 (1974).
16. B. P. J. Sandvik, "The Bainite Reaction in Fe–Si–C Alloys: The Primary Stage," Metall. Trans. A **13**, 777–787 (1982).
17. M. A. Shtremel', *Strength of Alloys. Part II. Deformation* (MISiS, Moscow, 1997) [in Russian].
18. M. P. Kashchenko and V. G. Chashchina, "Interpretation of Critical Cooling Rates of Alloy Steels Necessary for the Nucleation of Lamellar α Martensite in Dynamical Theory," in *Topical Problems of Metallography of Steels and Alloys* (Magnitogorsk. Gos. Tekhn. Univ., Magnitogorsk, 2012), pp. 104–105.
19. M. P. Kashchenko and V. G. Chashchina, "Critical Cooling Rates of Alloy Steels for the Nucleation of Lamellar α Martensite in a Dynamic Theory," Phys. Met. Metallogr. **113**, 893–901 (2012).
20. M. P. Kashchenko and V. G. Chashchina, "Formation of Bainitic Ferrite from the Viewpoint of the Dynamical Theory of Growth of Martensite Crystals," in *20th St. Petersburg Readings on the Problems of Strength* (St. Petersburg, 2012), part 2, pp. 77–79.